Improved prediction of soil properties with multi-target stacked generalisation on EDXRF spectra

Everton Jose Santana [a,*], Felipe Rodrigues dos Santos [b], Saulo Martiello Mastelini [c], Fábio Luiz Melquiades [b], Sylvio Barbon Jr [a]

[a] Department of Computer Science, State University of Londrina (UEL), Londrina, Brazil
[b] Department of Physics, State University of Londrina (UEL), Londrina, Brazil
[c] Institute of Mathematical Sciences and Computing, University of São Paulo (USP), São Carlos, Brazil

ARTICLE INFO

Keywords:
Machine learning
Multi-target regression
EDXRF Spectrometry
Soil quality

ABSTRACT

Energy dispersive X-ray fluorescence (EDXRF) is one of the most quick, environmentally friendly and least expensive spectroscopic analytical methodologies for assessing soil quality parameters. However, challenges in EDXRF spectral data analysis still demand more efficient methods. One possible solution is using Machine Learning (ML), particularly Multi-target Regression (MTR) methods, which predict multiple parameters taking advantage of inter-correlated parameters. In this study, we proposed the Multi-target Stacked Generalisation (MTSG), a novel MTR method relying on learning from different regressors in stacking structure for a boosted outcome. We compared MTSG and 5 MTR methods for predicting 10 parameters of soil fertility. Random Forest and Support Vector Regression (SVR) were used as learning algorithms embedded into each MTR method. Results showed the superiority of MTR methods over the Single-target Regression (the traditional ML method), reducing the predictive error for 5 parameters. Particularly, MTSG obtained the lowest error for phosphorus, total organic carbon and cation exchange capacity. When observing the relative performance of SVR with a radial kernel, the prediction of base saturation percentage was improved by 19%. Finally, the proposed method was able to reduce the average error from 0.67 (single-target) to 0.64 analysing all targets, representing a global improvement of 4.48%.

1. Introduction

Evaluation of soil management is of fundamental importance in modern agriculture to achieve an effective soil correction with focus on highly productive crops and high harvesting performance [1,2], as well as for supporting sustainable development [3]. In order to obtain such benefits, precision agriculture with proximal soil sensor (PSS) is an optimal solution and a tendency [4]. Non-destructive spectroscopic analytical methodologies coupled with machine learning have been studied to correlate the analytical signal to the soil fertility parameter of interest, including Visible/Infrared Spectroscopy [5–9] and X-ray Fluorescence (XRF) [10–13]. Particularly, XRF has been commonly used with benchtop equipment. However, with the advance in portable equipment, this analytical method may become a viable PSS technique for agriculture [14–18].

The Energy Dispersive XRF (EDXRF) is the modality that has been successfully applied for soil parameters analysis in different fields such as agronomy and environment (soil pollution) [19]. The EDXRF spectral data signal or the soil elemental concentrations are obtained faster, it is non-destructive, environmentally friendly, and is less expensive than the conventional methods. These features make EDXRF feasible as a PSS. However, analytical drawbacks such as poor performance for low-Z elements, matrix effects (due to moisture, granulometry, complex soil composition) and spectral interferences are challenges to be overcome with improvement in data collection and data analysis. In this paper we focus on data analysis, i.e., in the use of machine learning algorithms to pursuit high performance regression models for soil fertility parameters.

Commonly more than one parameter is involved in these analyses, forming an output set Y composed of d target variables. The traditional method to attack these problems is transforming the problem into d sub-problems with a single output variable, sharing the same input set X. This method is known as Single-target (ST) and serves as a baseline when

* Corresponding author.
E-mail addresses: evertonsantana@uel.br (E.J. Santana), fe.chicoo@gmail.com (F. Rodrigues dos Santos), mastelini@usp.br (S.M. Mastelini), fmelquiades@uel.br (F.L. Melquiades), barbon@uel.br (S. Barbon Jr).

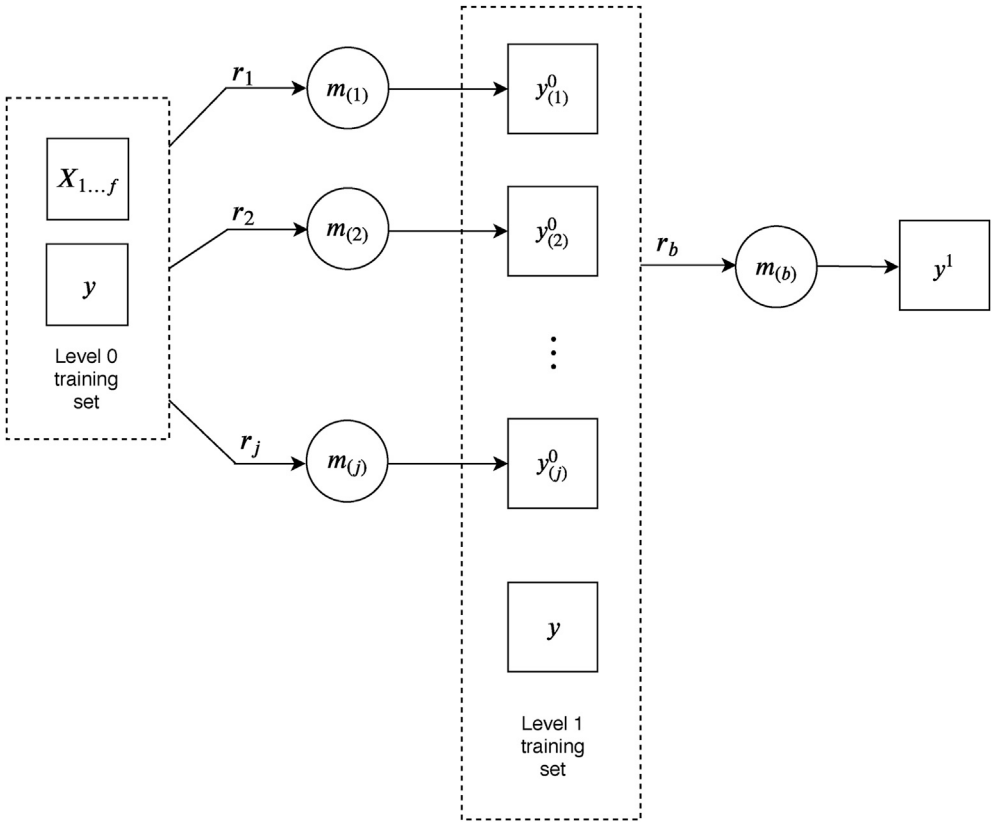

Fig. 1. Representation of SG ensemble technique.

referring to problems with multiple targets. In ST, independent individual models (regressors) are generated for each sub-problem considering the same input set X and the actual target.

Recent literature shows that new methods were developed especially to address multi-target settings. These methods, which are named Multi-target Regression (MTR) methods, oppose to ST by taking into account the correlation that the targets might have [20–24]. The MTR methods have been applied to different fields, as to predict vegetation condition, water quality and rock mass parameters, wheat flour quality and in soil assessment for heavy metal concentration [21,25–27]. Moreover, the prediction of multiple targets showed to be advantageous also for soil properties studies based on infrared data [28–30]. These results motivated the application and evaluation of MTR methods to handle soil samples analysed by EDXRF, which present difficulties of identification due to the complexity of the soil EDXRF spectra.

Besides applying existing MTR methods to this problem, in this work we developed a novel MTR method, Multi-target Stacked Generalisation (MTSG). Stacked Generalisation (SG) was the first stacking technique proposed in the literature, but it has not been explicitly addressed in the MTR tasks. As an ensemble technique, SG aims at combining the learning biases of different base-learners towards reducing the prediction error, specially if these regressors are dissimilar in their bias [31]. We believe this error reduction can also be achieved in the MTR field, particularly on EDXRF spectra, since the signal represents different properties and linearities from the same set of data. In other words, the proposed method is able to support the improved predictions of several targets taking advantage of different base-learner characteristics such as linearity, monotonicity and kernel function.

In short, this work aims at evaluating MTR methods in an EDXRF soil spectra dataset to predict 10 soil quality parameters and attest the best predictor for each target. Besides, it assesses the performance of the new method MTSG for minimising the prediction error. Random Forest and Support Vector Regression (with linear and radial kernels) were used as base learners for the methods.

After examining the motivation and novelty of this research, the work is organised as follows: Section 2 introduces the explored MTR methods and strategies. Section 3 describes MTSG, the new developed multi-target method. Following, Section 4 details the experimental setup, showing the dataset acquisition, the compared methods and algorithms, and the evaluation metrics. In Section 5, the results and their discussion are presented. Section 6 outlines the main conclusions of the work. Lastly, two appendices were added with the descriptive statistic of the soil parameters and the MTSG performance in benchmarking datasets.

2. Background

MTR methods can be split into several categories according to their training procedures [32]. Transforming the original problem into sub-problems is a well-grounded approach of MTR and it is based on two main strategies: stacking and chaining.

In stacking, one or more regressors are trained for each target (as in ST). They can be referred to as base-models. After that, predictions are obtained using the base-models for training a new regressor for each target in different manners. These new models, called meta-models, can be obtained following different stacking assumptions [21,33,34].

The precursor stacking MTR method was Stacked Single Target (SST), proposed by Ref. [21]. SST creates one base-model with a given regression algorithm (base-learner) for each target. Predictions are made by merging the output of base-models and the original input set, forming an augmented dataset. A new regressor is trained for each target taking into account the transformed dataset, generating d meta-models in the second layer.

[33] proposed the Deep Regressor Stacking (DRS) method, in which the stacking process of SST is repeated continuously, creating a deep meta-model. It stops when a maximum amount of pre-defined layers is reached.

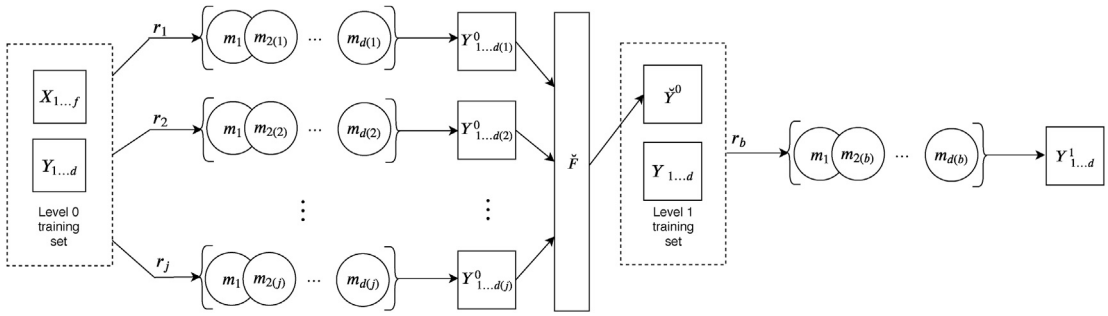

Fig. 2. Representation of MTSG method.

In another method, called Multi-target Augmented Stacking (MTAS), multiple distinct base-learners (related to different algorithms) are trained for each target using the same strategy as SST. However, the authors [34] took advantage of predictions for only relevant targets, obtaining boosted base-models. After that, just one final predictor per target is generated using the best set of augmented data, obtaining an accurate meta-model.

Chaining strategies, as the name implies, cascade the insertion of target-related information when creating new predictors. Similarly to stacking, chaining methods augment the original training set with predictions of the targets. Nonetheless, rather than using predictions of all responses at once, the chaining methods incrementally augment the datasets one target at the time. This idea is similar to the Bayesian network inference in design and was used initially for classification problems [35]. Different strategies were proposed in the recent MTR literature [21,36].

The Ensemble of Regressor Chains (ERC) constructs multiple randomly ordered target chains [21]. For each chain, base-models are trained for each target, starting from the first one. New regressors use the prediction of the previous base-models as extra input features. The final predictions for each target are accounted for as the average output among all chains.

Multi-output Tree Chaining (MOTC) [36] constructs a tree structure rather than multiple chains, where each node represents a target. To this end, a measure of inter-target correlation is used. Once the tree is constructed, starting from the leaves to the root, MOTC starts training the base-models. Each node uses its descendants' base-models predictions as extra outputs. Thus, a specialised chain based on a tree branch is created to improve each target prediction.

Our proposal follows the first strategy, stacking. Differently from the other mentioned methods, MTSG uses the original input set only in the first phase. After creating the first base-model and obtaining the predictions outputted by them, new base-models are created based only on those predictions as the input. Hence, MTSG not only models inter-target dependencies but also considers the learning strategies of different regressor algorithms to provide responses. This proposal will be detailed in the next Section.

3. Multi-target stacked generalisation

Ensemble methods were used in different tasks to improve predictive performance over single predictors [37,38]. In Ref. [39], for instance, stacking ensemble was adopted to predict soil organic matter. The wisdom of ensembles consists of the combination of different specialised components (with local minima) to produce a global minimum. Besides, these components can be obtained by different learning processes (either by different learning algorithms, parameters or training sets). The mentioned components can be classifiers or regressors, depending on the kind of problem. Since we deal with a regression problem, the specialised components in this work equal to regressors.

Ensemble approaches evolve generally two steps: ensemble generation step and integration step. The first occurs when the components are built and the second corresponds to when the output of the components are aggregated to generate a new prediction [40]. This aggregation can be made in different forms, for example, by a linear combination of the models.

Another strategy to integrate the specialised components is to obtain a model that has as input the prediction generated by the components, process known as Stacked Generalisation (SG) [41]. Fig. 1 represents SG technique.

SG consists of two main phases. The Level 0 training set is composed of the input set X with f features and the output variable y. Considering R as the set of possible regression algorithms, j elements of it ($r_1 \ldots r_j \in R$) will be used to obtain the base-models $m_{(1)} \ldots m_{(j)}$ for the targets.

After creating these base-models, the X set is used once again to obtain the first predictions (Y^0). The set of predicted targets Y^0 is then considered the new input set at Level 1.

In the second phase, one learning algorithm is chosen as the regressor (r_b). Thus, one Level 1 meta-model will be induced and considered the final predictor, and its prediction (y^1) will be considered the final output.

The Multi-Target Stacked Generalisation (MTSG) extends the SG concept to multiple outputs: whereas in original stacked generalisation multiple meta-models are trained for a single target, in MTSG multiple meta-models are trained for the multiple targets. Fig. 2 illustrates the MTSG design.

MTSG also has the generation and integration phases, increased by an intermediate pruning step made by a filter F. The Level 0 training set is composed of the input set X with f features and the output set Y with d targets. j base-learners will be used to obtain base-models for each target. In the first phase, j base-models m are induced for each target using the original training set.

The Level 0 base-models will be used along with the X set to obtain the first predictions (Y^0). Since j base-models are induced for each target at Level 0 and there are d targets, $j \times d$ values will be delivered for each instance at this level.

As an additional step, the set of predicted targets Y^0 will pass by the filter F. This filter will assess the relevance of the predictions in relation to each target and will preserve only the relevant ones for each target (Y^0). Those will be considered the new input set at Level 1. For performing the filtering, different metrics can be used (e.g. liner correlation among the targets). In this work, we adopted the importance extracted from Random Forest (RF), as in MTAS, since it is capable of modelling nonlinear relationships.

In the integration step, similarly to SG, one learning algorithm is chosen as the base-learner (r_b). In a supervised fashion, d Level 1 meta-models will be induced, i.e., there will be one new regressor ($m_{(b)}$) for each target. These will be considered the final models and their predictions ($Y^1_{1\ldots d}$) will be considered the final output of the method.

The training procedure of MTSG is shown in Algorithm 1. It receives X and Y, representing the input and output sets, respectively. R represents the set of base-learners that will be used at Level 0 and r_b represents the base-learner employed to create the final meta-models.

Algorithm 1. MTSG training algorithm.

Algorithm 1 MTSG training algorithm

function MTSG(X, Y, R, r_b)
  // To store the Level 0 predictions
  $Y^0 \leftarrow \{\}$
  // Level 0 base-models
  Level $0 \leftarrow \{\}$
  // Regression model induction for each target and learner
  for $r \in R$ **do**
    for t = 1 **to** d **do**
      // model induction
      $m_{t(r)} : X \xrightarrow{r} Y_t$
      $Y^0_{t(r)} \leftarrow \text{predict}(m_{t(r)}, X)$
      Level $0_{t(r)} \leftarrow m_{t(r)}$
  // Second layer of meta-models
  $\text{Level}_1 \leftarrow \{\}$
  for t = 1 **to** d **do**
    $X' \leftarrow \breve{Y}^0_t$
    $m_{t(b)} : X' \xrightarrow{r_b} Y_t$
    Level $1_t \leftarrow m_{t(b)}$
  $mtsg \leftarrow \{\text{Level 0, Level 1}\}$
return $mtsg$

In this method, the original problem's features are disregarded at Level 1. To the best of our knowledge, this represents a distinction when comparing to the other multi-target stacking methods of the literature.

Besides, since it is an ensemble method, the performance of MTSG is sensitive to the diversity achieved by the Level 0 regressors. Using more learning algorithms tends to bring more diversity, however it increases the complexity of the method. For this reason, the number and type of regressors that will be used represent the compromise between performance and complexity in MTSG.

4. Experimental setup

4.1. EDXRF working principle

EDXRF is a technique used in several study fields for identification and quantification of chemical elements present in varied materials, for instance vegetables [42], bee honey [43], archaeological objects [44], dog hair [45] and soils [46–48]. The working principle of EDXRF depends on the interaction of high-energy X-rays with matter. These interactions may be performed by photoelectric effect, elastic and inelastic

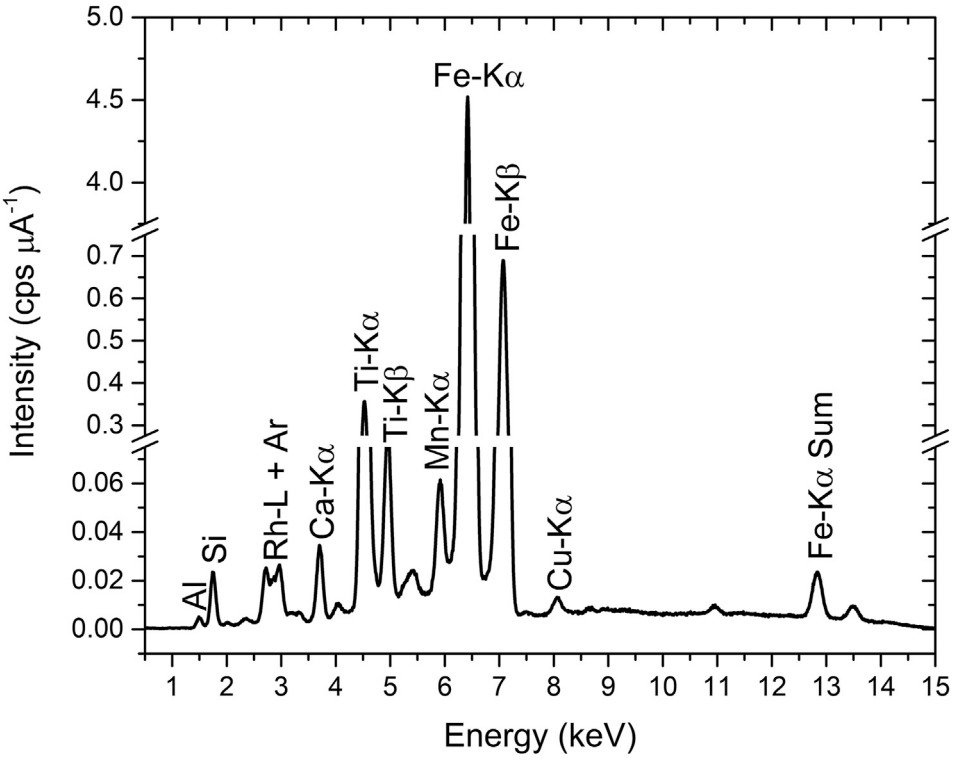

Fig. 3. Mean EDXRF spectra of the analysed soil.

scattering [49]. The fluorescent phenomenon is related to the photoelectric effect in which electrons are ejected from inner shells of the atom by the incidence of an external X-ray beam. As a consequence, to stabilise the atom, electrons from external layers fill these vacancies and the energy difference is emitted as characteristic X-ray photons. Thus, it is possible to identify the elements present in the sample since these energies differences are well defined for each transition in each element. By evaluating the peak intensities in the spectra, the elemental concentrations may be calculated [49]. Besides the total inorganic content, the EDXRF spectra also provide some information about the complex organic content. The inorganic and organic samples' information is mainly embodied in the spectra scattering region since the cross-section of the scattering effects is greater for low Z-elements.

4.2. Conventional analyses and spectral measurements

Soil samples (n = 396) from an agricultural area in *Ribeirão Vermelho* basin in Cambé municipality, Paraná State, Brazil (north region of Paraná state) were used in this study. The area has two types of soil classified as *Latossolo Vermelho Amarelo Distrófico* (Orthic Ferralsol) and *Nitossolo Vermelho Distrófico*, according to the Brazilian classification system and FAO classification [50,51], both with high clay texture. Samples were collected in three depths (0–5 cm, 5–10 cm and 10–20 cm), dried at 40 °C for 48 h, grinded and sieved through a 2 mm stainless steel sieve. Next, soil samples were sent to laboratory for conventional analysis of the chemical parameters and EDXRF spectral measurements.

The soil fertility parameters analysed were: bioavailable phosphorus (P), total organic carbon (TOC), pH, potential acidity ($H^{+} + Al^{3+}$, that will be denoted by H+Al for simplification purpose), Ca^{+2} (Ca), Mg^{+2} (Mg), K^{+} (K), sum of exchange bases (SB), cation exchange capacity (CEC) and base saturation percentage (BSP). TOC was determined by dichromate-oxidation method (Walkley-Black). Ca and Mg were obtained by *KCl* 1 mol L^{-1}, with the solution being measured by atomic absorption spectrometry. Using a Mehlich-1 extraction solution, K and P were acquired by flame spectroscopy and UV–Vis molecular absorption spectrophotometry. pH measurements were made using a potentiometer in $CaCl_2$ solution in 1:2.5 proportion. Adding an SMP buffer solution, the readings of pH-SMP were employed to determine H+Al.

SB corresponds to the sum of Ca, Mg and K. CEC was set as the sum of Ca, Mg, K and H+Al. Ultimately, BSP was given by:

$$BSP = \frac{100 \times SB}{CEC}. \tag{1}$$

All analyses were executed in the IAPAR Soil Analysis Laboratory in Londrina, Paraná, Brazil following the recommendations of [52]. The statistical analysis of these measurements can be observed in Appendix A.

The EDXRF measurements were carried out in the Shimadzu (EDX720 model) benchtop equipment with Rh X-ray tube. For this, 5 g of samples were placed in XRF plastic cups covered with Mylar films. The measurements were repeated three times in different sample portions (shaking the XRF cup before each measurement) using the operation condition of 15 kV for 200 s. The detection was carried out using a Si (Li) detector cooled with liquid nitrogen. All samples were measured using 10-mm focal spot without any filter in the primary beam. The mean EDXRF spectra are presented in Fig. 3.

4.3. Methods and algorithms

The use of machine learning tools may help to work around and minimise the analytical drawbacks mentioned in the introduction and also perform rapid dataset analyses for soil characterisation [11,53].

The original dataset was split into two sub-sets following Kennard–-Stone algorithm. 2/3 of the samples were reserved for training and 1/3 for test. This resulted in a hold-out validation training set containing 264 examples and a test set containing 132 examples (that were unseen during the whole training). The samples were further pre-processed using z-transform, also known as auto-scaling [54].

Table 1
Main default hyperparameters of RF, SVM_L and SVM_R in the packages *ranger* and *e1071*.

Regressor	Hyperparameter	Value
RF	number of trees	500
	mtry	(rounded down) square root of the number of variables
	minimum node size	5
	maximum depth	None
	split rule	variance
SVR_L	ε	0.1
	tolerance	0.001
	regularization	1
SVR_R	ε	0.1
	tolerance	0.001
	regularization	1
	γ	1/(data dimension)

ST was compared to SST, ERC, MTAS, MOTC, DRS and the novel method, MTSG. Random Forest (RF) and Support Vector Regression (SVR) were used as Level 0 and base regressors in this work. All methods along with the base regressors were implemented in R 3.4.0 with default settings, and the implementation can be accessed in.[1] The packages used for RF and ε-insensitive SVR were *ranger*[2] and *e1071*,[3] respectively. The main default hyperparemeters stated in these packages for each regressor are shown in Table 1.

RF creates multiple decision trees considering subsets of training set features, forming a forest with specialised trees. The output of RF, when applied to regression problems, is the average of the trees in the forest.

SVR creates a hyperplane that minimises the training error. When using a linear kernel (SVR_L), it creates a linear function to accomplish the task of minimising the error. When using a radial kernel (SVR_R), it maps the training data to a higher dimension via a radial function and then finds a hyperplane that best minimises the error.

These algorithms were chosen due to the relevant performance in previous studies and to guarantee a diversity to ensemble, since they are grounded in different strategies to tackle the problem. We limited the number of algorithms and used the default parameters in a sense of fairness with the compared algorithms and MTR methods, and to avoid the use of excessive computational resources.

4.4. Evaluation metrics

For analysing the quality of the methods concerning the prediction of each soil variable, the Root Mean Squared Error (RMSE) of each target t was calculated between the predicted value (y_t) and the true value of the target ($\hat{y}_t$) for the N testing instances. It indicates the concentration of the data in relation to the fitting model [55]:

$$RMSE_t = \sqrt{\frac{\sum_{i=1}^{N}\left(y_t^i - \hat{y}_t^i\right)^2}{N}} \tag{2}$$

Still focusing on the performance for each target, the multi-target methods can be compared to the single-target by the Relative Performance per Target (RPT), in which a value greater than 1 is a synonym of improved performance of a specific MTR method in relation to the ST method:

$$RPT_{MTR,t,r} = \frac{RMSE_{ST,t,r}}{RMSE_{MTR,t,r}} \tag{3}$$

[1] http://www.uel.br/grupo-pesquisa/remid/?page_id=145.
[2] https://cran.r-project.org/web/packages/ranger/ranger.pdf.
[3] https://cran.r-project.org/web/packages/e1071/e1071.pdf.

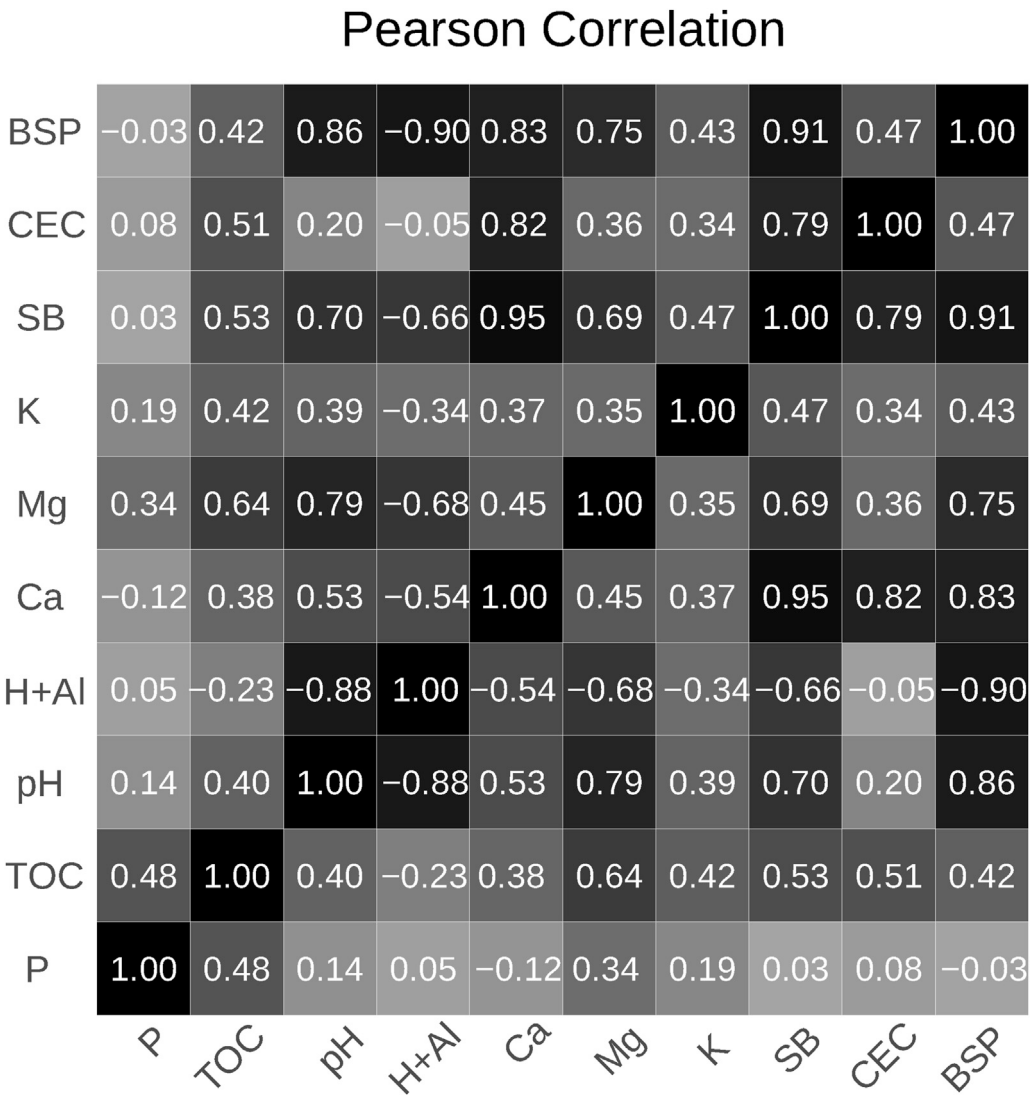

Fig. 4. Pearson correlation coefficients among the 10 targets.

For this problem, t corresponds to each soil parameter and r, to the base learner.

To compare the performance of different methods for different problems, it is necessary a metric that can be computed regardless of the number of targets d. The general performance of each method can be computed by the average Relative Root Mean Square Error (aRRMSE) [20]:

$$aRRMSE_{MTR} = \frac{1}{d}\sum_{t=1}^{d}\sqrt{\frac{\sum_{i=1}^{N}(y_t^i - \hat{y}_t^i)^2}{\sum_{i=1}^{N}(y_t^i - y)^2}} \tag{4}$$

A complementary metric to access the performance of the best models related to the reference values is the ratio of performance to deviation (RPD) which is the ratio of the standard deviation (SD) of the conventional analysis (reference) to the RMSE of the prediction:

$$RPD = \frac{SD}{RMSE} \tag{5}$$

According to Ref. [56], for soil attributes RPD < 1.0 indicates very poor predictions and their use is not recommended; RPD between 1.0 and 1.4 indicates poor predictions where only high and low values are distinguishable; RPD between 1.4 and 1.8 indicates fair predictions which may be used for assessment and correlation; RPD values between 1.8 and 2.0 indicates good predictions where quantitative predictions are possible; RPD between 2.0 and 2.5 indicates very good, quantitative predictions, and RPD > 2.5 indicates excellent predictions.

Additionally, the quality of the predictions can be given by the ratio of performance to interquartile (RPIQ). RPIQ is based on quartiles, which better represent the spread of the population. It is defined as the ratio of the distance between the third quartile (Q3) and the first (Q1) to RMSE:

$$RPIQ = \frac{Q3 - Q1}{RMSE} \tag{6}$$

This metric better accounts for the spread of the population and large RPIQ values indicate improved model performance [57].

5. Results and discussion

The results were presented and discussed starting by exposing the correlation between the targets (Section 5.1). This information corroborates with the importance of applying MTR methods since correlated targets lead to reduced errors in MTR predictions. Afterwards, in Section 5.2, we present the results of ST and MTR methods, highlighting the contribution of MTSG, which overcame the other methods. Finally, the predictions of each soil property are compared for evaluating their

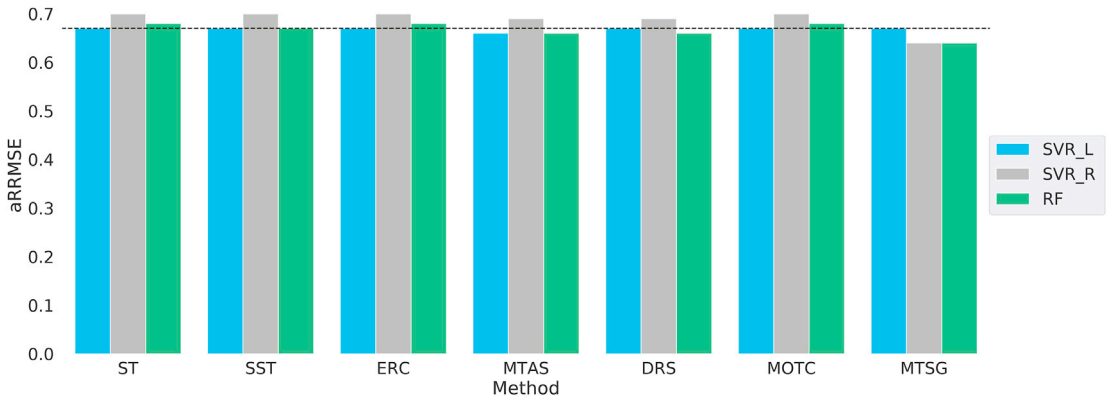

Fig. 5. aRRMSE for the different combinations of methods and regressors. The horizontal line represents the lowest aRRMSE for ST.

Table 2
RPT for each target considering the different combinations of methods and regressors. The best average result of each regressor is highlighted in bold.

	Regressor	P	TOC	pH	H+Al	Ca	Mg	K	SB	CEC	BSP	Average
RPT_{SST}	SVR_L	1.00	1.00	1.00	1.00	1.00	1.00	1.00	1.00	1.00	1.00	1.00
RPT_{SST}	SVR_R	1.00	1.04	1.00	1.00	1.00	1.00	1.00	1.00	1.00	1.01	1.01
RPT_{SST}	RF	1.01	1.00	1.00	1.00	1.13	1.00	1.00	1.10	1.00	1.03	1.03
RPT_{ERC}	SVR_L	1.00	1.00	1.00	1.00	1.00	1.00	1.00	1.00	1.00	1.00	1.00
RPT_{ERC}	SVR_R	1.00	1.04	1.00	1.00	1.00	1.00	1.00	1.00	1.00	1.00	1.00
RPT_{ERC}	RF	1.01	1.00	1.00	1.00	1.13	1.00	1.00	1.10	1.00	1.02	1.03
RPT_{MTAS}	SVR_L	1.01	1.05	1.00	1.00	1.00	1.00	1.00	1.00	1.13	1.03	**1.02**
RPT_{MTAS}	SVR_R	1.01	1.04	1.00	1.00	1.00	1.00	1.00	1.00	1.00	1.04	1.01
RPT_{MTAS}	RF	1.03	1.04	1.00	1.00	1.13	1.00	1.00	1.10	1.00	1.03	1.03
RPT_{MOTC}	SVR_L	1.00	1.00	1.00	1.00	1.00	1.00	1.00	1.00	1.00	1.00	1.00
RPT_{MOTC}	SVR_R	1.00	1.04	1.00	1.00	1.00	1.00	1.00	1.00	1.00	1.00	1.00
RPT_{MOTC}	RF	1.00	1.00	1.00	1.00	1.00	1.00	1.00	1.10	1.00	1.03	1.01
RPT_{DRS}	SVR_L	1.00	1.00	1.00	1.00	1.00	1.00	1.00	1.00	1.00	1.00	1.00
RPT_{DRS}	SVR_R	1.01	1.04	1.00	1.00	1.00	1.00	1.00	1.00	1.00	1.04	1.01
RPT_{DRS}	RF	1.01	1.00	1.00	1.00	1.13	1.00	1.00	1.10	1.00	1.08	1.03
RPT_{MTSG}	SVR_L	1.00	1.00	1.00	1.00	1.00	1.00	1.00	1.00	1.00	1.00	1.00
RPT_{MTSG}	SVR_R	1.06	1.14	1.00	1.11	1.13	1.00	1.11	1.10	1.13	1.19	**1.10**
RPT_{MTSG}	RF	1.08	1.14	1.00	1.00	1.13	1.00	1.00	1.10	1.13	1.00	**1.06**

predictive performance and bring insights from patterns of EDXRF spectra in Section 5.3.

5.1. Soil properties correlation

Fig. 4 reveals the Pearson correlation coefficients among the targets. They were computed pair-wisely based upon the experimented dataset and the closer to 1 or -1, the higher the linear correlation between the two variables [58]. Coefficients closer to 0 means a low correlation.

As observed, several targets are strongly correlated: Ca and SB result in the most expressive coefficient since they presented a correlation coefficient of 0.95, almost a perfect positive linear correlation. Other targets pairs that are strongly correlated are BSP and SB (0.91), BSP and pH (0.86), BSP and Ca (0.83), CEC and Ca (0.82), and Mg and pH (0.79). The targets BSP and H+Al presented a negative strong correlation (−0.90). The mostly uncorrelated targets were P and SB (0.03), P and BSP (−0.03), P and H+Al (0.05), and P and CEC (0.08). In fact, P was the most uncorrelated target among the other nine.

5.2. Multi-target prediction

Fig. 5 shows the aRRMSE for all methods and base-learners. For this, the lower the value, the better the performance. Comparing the base-learners with the average error of all targets, SVR_L was an effective machine learning algorithm, obtaining the same performance in all methods (ST and MTR, except for MTAS). SVR_R and RF were able to reduce the average error only when used embedded in DRS, MTAS and MTSG.

With ST, the lowest aRRMSE was obtained using SVR with a linear kernel, resulting in an aRRMSE of 0.67. Despite of introducing non linearities, the MTSG presented a significative improvement in the predictive power of the models. MTSG using SVR with a radial kernel and RF as base regressor led to the lowest aRRMSE, 0.64. Other improvements in relation to the lowest ST value were obtained by DRS using RF (0.66), MTAS with SVR_L (0.66) and MTAS with RF (0.66). It is remarkable that these base learners are using default hyperparameters, and these results could be improved by tuning them. However, searching for optimal hyperparameters increases the complexity of the methods and could influence the stacking performance.

After evaluating the general error results of the methods, their performances were evaluated for each target in terms of RPT, as registered in Table 2. For this metric, values greater than 1 represent an improvement of MTR over ST.

For P, TOC, pH, H+Al, Ca, Mg, K, SB, CEC and BSP, i.e., all the targets, all the combinations of MTR methods obtained improved or at least equivalent performance with respect to their corresponding ST version. Notably, many improvements reached up to around 10% (using MTSG) in relation to the corresponding ST. When observing the average RPT (last column in Table 2), just MTAS was able to improve results using SVR_L. It may also be noted in Table 1 that RF generated a performance improvement in all the MTRs in relation to ST for SB.

5.3. Soil properties prediction

Continuing the discussion for individual targets, we present (Fig. 6) the absolute error values between the ST and the MTR methods for each

Fig. 6. RMSE values for each target considering the different combinations of methods and base-learners. The horizontal lines represent the lowest RMSE for ST related to each target.

Table 3
RMSE, RPD and RPIQ performances of the best models for each target.

Target	Best model(s)	RMSE	RPD	RPIQ
P (mg kg^{-1})	MTSG (RF)	7.6	1.2	1.6
TOC (g kg^{-1})	MTSG (SVR_R, RF)	2.1	2	3.1
pH	All models	0.3	1.3	1.6
H+Al ($cmol_c$ kg^{-1})	Several models	0.9	1.3	1.5
Ca ($cmol_c$ kg^{-1})	Several models	0.8	1.9	3.0
Mg ($cmol_c$ kg^{-1})	All models	0.4	1.5	2.0
K ($cmol_c$ kg^{-1})	MTSG (SVR_R)	0.09	1.3	2.3
SB ($cmol_c$ kg^{-1})	Several models	1	1.9	2.5
CEC ($cmol_c$ kg^{-1})	MTAS (SVR_L), MTSG (SVR_R, RF)	0.8	1.9	2.8
BSP (%)	DRS (RF)	6.1	1.8	1.9

target. For all the targets, except for BSP, ST models presented the lowest RMSE using SVR_L, and it indicates a linear relationship between the EDXRF spectral data and the studied targets.

Two properties, pH and Mg, did not improve their predictive performances through the use of MTR. For pH and Mg, all base-learners (SVR_L, SVR_R and RF) provided the same lowest RMSE in ST and MTR methods, respectively 0.3 and 0.4 $cmol_c$ kg^{-1}. When targets have low or even none correlation among the other targets, it is possible to affirm these targets hardly have their performances improved by using MTR techniques. On the other hand, some cases with average or strong correlation without predictive performance improvements reveal the data's limit to describe the specific target. In our experiments, we observed the EDXRF spectra had already obtained the optimal performance when describing the pH and Mg exposing likely description boundaries on these soil properties.

For all the other properties, at least one meta-model had reduced error in comparison to ST. Regarding K, all ST and MTR methods obtained 0.10 $cmol_c kg^{-1}$, except our proposal. MTSG (SVR_R) was able to reduce the error to 0.09 $cmol_c kg^{-1}$. For P, SVR_L provided the lowest RMSE in ST method (7.8 mg kg^{-1}). Considering P and MTR methods, MTSG with RF was able to reduce this error to 7.6 mg kg^{-1}. For TOC, SVR_L provided the lowest RMSE in ST method (2.3 g kg^{-1}). Regarding TOC and MTR methods, MTSG with SVR_R and RF was able to reduce the error to 2.1 g kg^{-1}. Dealing with H+Al, SVR_L and RF provided the lowest RMSE in ST method (0.9 $cmol_c kg^{-1}$). About MTR methods and this property, SVR_L and RF achieved the same error (0.9 $cmol_c kg^{-1}$). MTSG with SVR_R was also able to achieve this value. When predicting Ca, SVR_L provided the lowest RMSE in ST method (0.8 $cmol_c$ kg^{-1}). Using MTR methods, SST, ERC, MTAS and DRS with SVR_L and RF achieved the same error (0.8 $cmol_c$ kg^{-1}). MOTC achieved this error only using SVR_L and MTSG achieved this error with RF, SVR_L and SVR_R. Regarding SB, SVR_L provided the lowest RMSE in ST method (1.0 $cmol_c$ kg^{-1}). Considering MTR methods, SVR_L and RF achieved the same error (1.0 $cmol_c$ kg^{-1}). MTSG with SVR_R was also able to achieve this value. For CEC, SVR_L, SVR_R and RF provided the lowest RMSE in ST method (0.9 $cmol_c$ kg^{-1}). Considering MTR methods, MTAS with SVR_L and MTSG with SVR_R and RF were able to reduce the error to 0.8 $cmol_c$ kg^{-1}. Finally, regarding BSP, RF provided the lowest RMSE in ST method (6.6%). Considering MTR methods, DRS with RF was able to reduce the error to 6.1%.

To summarise, in ST method, for pH and Mg, all base-learners shared the same RMSE. RF alone presented the lowest error in ST only for BSP. Thus, for ST method, SVR_R was not the unique best regressor for any of the targets, and there is a prevalence of SVR_L. This scenario, however, changed when these regressors were used as base-learners for the MTR methods: ignoring the cases that MTR did not bring improvements to ST, RF was present as the base-learner for 4 targets (P, TOC, CEC and BSP), SVR_R for 3 targets (TOC, K and CEC) and SVR_L for 1 target (CEC). This shows that the modifications inherent to MTR methods introduced non-linearity to the data.

P is one target that was favoured by this non-linearly: the Pearson correlation coefficients of P with other targets, as discussed in Fig. 4, revealed that it was least linearly correlated to other targets. Nonetheless, its RMSE lowered with MTSG coupled with RF.

As observed, the best MTR methods resulted in RMSE values at least equivalent to ST. For the targets pH, H+Al, Ca, Mg and SB, none of the MTR methods improved the performance, so ST would be preferable to predict them due to the lower complexity. On the other hand, for the other 5 targets, at least one MTR method improved the performance, specially MTSG, but also DRS and MTAS.

In order to evaluate the accuracy of the best models for each target related to the conventional methods, the RPD for the predictions were calculated (Table 3). The standard deviation data used for RPD calculation is on Appendix A, as well as the data needed for calculating the interquartile distance in RPIQ.

According to RPD, the targets that presented poor prediction, where only high and low values are distinguishable, were P, pH, H+Al and K. These targets had low prediction performance with EDXRF sensor due to its low detection sensibility for light elements. For Mg, the models obtained fair predictions, indicating the viability of the method. BSP is in the threshold of fair and good predictions. Ca, SB and CEC presented good predictions. Finally, TOC is in the threshold between good and very good quantitative predictions. In this sense, six relevant parameters used for evaluating soil quality obtained at least fair predictions in relation to conventional methods.

The RPIQ results agree with the RPD values, showing that most of the targets had at least one satisfactory model for quantitative predictions. In particular, TOC, Ca and CEC delivered the greatest RPIQ. For the three parameters, MTSG was included among the best model.

6. Conclusion

In this work, we evaluated the usage of MTR methods to predict 10 soil parameters based on EDXRF as input information. We also developed MTSG, a novel MTR method. In relation to the aRRMSE, MTR methods were able to reduce the error over ST, especially MTAS, DRS and MTSG. Concerning RPT, for all targets, all MTR methods were better than or equal to their respective regressor version in ST.

MTSG was the best method for predicting the soil characteristics of the studied problem, obtaining the lowest RMSE for 4 out of the 10 targets and was able to reduce the baseline aRRMSE from 0.67 to 0.64, representing a global improvement of 4.48%. In the best target improvement, i.e. BSP, the proposed method boosted in 19% the predictive performance using SVR_R baseline.

Finally, the comparison to reference methods showed that the MTR predictions were at least fair for 6 targets. Among them, when using MTSG, TOC delivered the best overall RPD and RPIQ. Based on the results, MTR is capable of improving the prediction of soil properties, with a special highlight to MTSG. Notwithstanding, one of the limitation of this method is the low interpretability.

As future work, we will investigate the use of MTSG with more different base-learners when creating the base-models, even the meta-model, since it was observed suitable algorithms for particular targets. Optimising the regressors hyperparameters and investigating their influence in the stacking performance is also a research path. Besides, the combination of different types of PSS and additional available MTR methods may offer a viable solution for direct soil analysis, and it can be further explored. Another possibility is performing spectral pre-treatments to the input data. Lastly, the use of MTSG to analyse other types of soils and applying the compared methods in larger spectral libraries is also encouraged.

Author statement

Everton Jose Santana: Writing - Original Draft, Visualization, Investigation, Formal analysis; **Felipe Rodrigues dos Santos:** Writing - Original Draft, Visualization, Resources, Data Curation; **Saulo Martiello Mastelini:** Writing - Review & Editing, Software, Methodology; **Fábio**

Luiz Melquiades: Writing - Review & Editing, Supervision, Resources, Data Curation; **Sylvio Barbon Jr.** : Writing - Review & Editing, Supervision, Conceptualization, Project administration.

Declaration of competing interest

The authors declare that they have no known competing financial interests or personal relationships that could have appeared to influence the work reported in this paper.

Acknowledgement

This study was financed in part by the Coordenação de Aperfeiçoamento de Pessoal de Nível Superior - Brasil (CAPES) - Finance Code 001, CNPQ (grants #420562/2018-4, #142985/2016-3 and #304722/2017-0), São Paulo Research Foundation (FAPESP) grant #2018/07319-6 and Fundação Araucária (Brazilian Agencies). We would like to thank Dr. Graziela M.C. Barboza, Dr. José Francirlei de Oliveira and IBITIBA research project (32.02.120.00.00) for the support in sample collection and conventional analysis.

Appendix A. Descriptive statistics of the soil parameters

Table 4 presents the descriptive statistics of the soil parameters determined by conventional analysis for all samples, calibration set and prediction set.

Table 4
Result of descriptive statistics of soil parameters determined by conventional methods. SD represents standard deviation and CV, coefficient of variation.

Parameters	Mean ± SD	CV (%)	Median	Minimum	Maximum	1st Quartile	3rd Quartile	Skewness	Kurtosis
All samples (n = 396)									
TOC (g kg-1)	19.8 ± 4.1	22	20.2	7.6	30.5	16.8	23.1	−0.27	−0.49
pH	5.3 ± 0.4	8	5.2	4.2	6.5	5.0	5.5	0.32	0.13
H+Al (cmolc kg-1)	5.4 ± 1.1	20	5.3	2.7	9.7	5.0	6.2	0.29	0.80
Ca (cmolc kg-1)	6.0 ± 1.5	25	6.2	1.4	9.2	4.9	7.2	−0.43	−0.49
Mg (cmolc kg-1)	2.0 ± 0.6	28	2.0	0.7	3.7	1.6	2.4	0.56	−0.24
K (cmolc kg-1)	0.24 ± 0.16	67	0.18	0.05	1.15	0.12	0.30	1.56	3.48
P (mg kg-1)	13.9 ± 9.9	71	12.3	0.4	69.8	6.9	18.9	1.72	5.35
SB (cmolc kg-1)	8.2 ± 1.9	23	8.4	2.1	12.6	7.1	9.6	−0.52	−0.17
CEC (cmolc kg-1)	13.7 ± 1.5	11	13.8	9.3	17.9	12.6	14.9	−0.21	−0.31
BSP (%)	60 ± 10	18	61	18	80	55	66	−0.91	1.56
Calibration set (n = 264)									
TOC (g kg-1)	20.0 ± 4.4	22	20.4	7.6	30.5	16.8	23.1	−0.27	−0.47
pH	5.3 ± 0.4	8	5.2	4.2	6.5	5.0	5.5	0.34	0.09
H+Al (cmolc kg-1)	5.4 ± 1.0	19	5.3	2.7	9.0	5.0	6.2	0.00	0.31
Ca (cmolc kg-1)	6.1 ± 1.5	24	6.2	1.4	9.2	4.9	7.1	−0.46	−0.47
Mg (cmolc kg-1)	2.1 ± 0.6	28	1.9	0.7	3.5	1.6	2.4	0.60	−0.37
K (cmolc kg-1)	0.25 ± 0.17	68	0.18	0.05	1.15	0.12	0.30	1.73	4.67
P (mg kg-1)	14.1 ± 10.2	72	13.1	0.4	69.8	6.5	18.7	1.85	6.55
SB (cmolc kg-1)	8.4 ± 1.8	22	8.5	2.2	12.6	7.1	9.6	−0.53	−0.22
CEC (cmolc kg-1)	13.8 ± 1.6	11	13.8	9.3	17.9	12.5	14.9	−0.21	−0.32
BSP (%)	60 ± 9	15	61	20	80	55	66	−0.74	1.19
Prediction set (n = 132)									
TOC (g kg-1)	19.4 ± 4.2	22	19.7	9.5	29.2	16.5	22.9	−0.27	−0.51
pH	5.3 ± 0.4	8	5.2	4.2	6.5	5.0	5.5	0.30	0.24
H+Al (cmolc kg-1)	5.5 ± 1.2	22	5.3	3.1	9.7	5.0	6.2	0.86	1.60
Ca (cmolc kg-1)	5.6 ± 1.5	27	6.0	1.4	8.7	4.8	7.2	−0.38	−0.50
Mg (cmolc kg-1)	2.0 ± 0.6	30	2.0	0.6	3.7	1.7	2.4	0.48	0.13
K (cmolc kg-1)	0.20 ± 0.12	60	0.20	0.05	0.65	0.12	0.33	1.23	1.13
P (mg kg-1)	13.5 ± 9.4	70	11.1	0.6	55.0	7.4	19.3	1.44	2.82
SB (cmolc kg-1)	7.9 ± 1.9	24	8.3	2.1	11.9	7.2	9.7	−0.51	−0.03
CEC (cmolc kg-1)	13.4 ± 1.4	11	13.7	9.4	17.2	12.8	15.0	−0.19	−0.35
BSP (%)	58 ± 11	18	61	18	77	54	66	−1.23	2.30

Appendix B. General comparison of MTSG with other methods

MTSG is being first proposed in this work. To validate this method, MTSG performance was assessed in benchmarking datasets commonly used in MTR literature.

These datasets enclose different kind of problems, as shown in Ref. [21]: air ticket prices (atp1d and atp7d), machining parameter settings (edm), solar flares types (sf1 and sf2), heavy metals concentration in soil (jura), energy efficient buildings requirements (enb), concrete properties (slump), water quality properties (andro) and online engagement (scpf).

The aRRMSE resulting of the usage of ST, SST, ERC, MTAS, MTSG, MOTC and DRS with the base learners RF and SVR_R for these datasets are presented in Table 5. The average rankings obtained by each of the MTR methods are also presented at the bottom of the table for visual clarity.

Table 5
aRRMSE comparison among the methods for literature benchmarking datasets. The bold values correspond to the smallest aRRMSE per dataset for each learning algorithm.

Dataset	ST		SST		ERC		MTAS		MOTC		DRS		MTSG	
	RF	SVR_R	RF	SVR_R	RF	SVR_R	RF	SVR_R	RF	SVR_R	RF	SVR_R	RF	SVR_R
atp1d	0.3927	0.4291	0.3889	0.4290	0.3898	0.4290	**0.3841**	**0.4170**	0.4064	0.4627	0.3894	0.4311	0.3935	0.4230
atp7d	0.5108	0.6169	0.5041	0.6166	0.5094	0.6169	0.5107	0.5983	0.5844	0.7805	**0.5025**	0.6159	0.5250	**0.5877**
edm	0.6668	0.7400	0.7146	0.7321	**0.6620**	0.7355	0.6852	0.6779	0.6655	0.8761	0.6799	0.7489	0.7404	**0.6691**
sf1	0.8749	0.8054	1.0145	0.8131	0.9078	**0.8013**	1.0347	0.8167	**0.8723**	0.9938	0.8744	0.8040	1.0499	1.0001
sf2	**0.8254**	0.7840	0.8955	0.7878	0.8399	0.7851	0.9150	0.7894	0.8280	1.5992	0.8303	**0.7829**	0.9324	1.4815
jura	0.5842	0.6210	0.5734	0.6240	0.5752	0.6202	**0.5673**	**0.5997**	0.5792	0.6967	0.5758	0.6280	0.5739	0.6596
enb	0.1504	0.2510	0.1145	0.2190	0.1293	0.2415	**0.1085**	**0.1236**	0.1169	0.3171	0.1129	0.1688	0.1162	0.2017
slump	0.8293	0.7348	0.8484	0.7510	0.8182	0.7293	0.8159	0.8165	**0.7633**	**0.7039**	0.8654	0.7364	0.7982	0.7487
andro	0.8131	1.1912	0.7330	1.0197	0.7886	1.0929	0.5952	0.8980	0.5568	1.1806	**0.5435**	0.7713	0.6078	**0.6009**
scpf	0.8683	0.8190	0.8533	**0.8016**	**0.8321**	0.8060	0.9466	2.5352	0.8701	3.3978	0.8444	0.8026	0.8793	0.8033
Average rank	7.20	8.50	6.60	7.80	6.20	7.70	6.20	7.90	5.90	12.20	**5.40**	7.30	8.10	8.00

As observed, none of the methods is the best for all the problems. MTAS presented the lowest performance in 3 datasets for both RF and SVR_R. ERC, MTSG, MOTC and DRS presented the lowest aRRMSE for 3 datasets each, depending on the base regressor. SST and ST were able to minimise the aRRMSE once each.

To conclude, the result shows that MTSG performance is comparable to previous proposed methods. Also, depending on the problem, its performance can be superior to the other methods.

References

[1] M. Suchithra, M.L. Pai, Improving the prediction accuracy of soil nutrient classification by optimizing extreme learning machine parameters, Inf. Process. Agric. 7 (1) (2020) 72–82.

[2] L. Montanarella, D.J. Pennock, N. McKenzie, M. Badraoui, V. Chude, I. Baptista, T. Mamo, M. Yemefack, M. Singh Aulakh, K. Yagi, S. Young Hong, P. Vijarnsorn, G.-L. Zhang, D. Arrouays, H. Black, P. Krasilnikov, J. Sobocká, J. Alegre, C.R. Henriquez, M. de Lourdes Mendonça-Santos, M. Taboada, D. Espinosa-Victoria, A. AlShankiti, S.K. AlaviPanah, E.A.E.M. Elsheikh, J. Hempel, M. Camps Arbestain, F. Nachtergaele, R. Vargas, World's soils are under threat, SOIL 2 (1) (2016) 79–82.

[3] J. Bouma, L. Montanarella, G. Evanylo, The challenge for the soil science community to contribute to the implementation of the UN sustainable development goals, Soil Use Manag. 35 (4) (2019) 538–546.

[4] T. Angelopoulou, A. Balafoutis, G. Zalidis, D. Bochtis, From laboratory to proximal sensing spectroscopy for soil organic carbon estimation — a review, Sustainability 12 (2) (2020) 443.

[5] Y. Wang, T. Huang, J. Liu, Z. Lin, S. Li, R. Wang, Y. Ge, Soil pH value, organic matter and macronutrients contents prediction using optical diffuse reflectance spectroscopy, Comput. Electron. Agric. 111 (2015) 69–77.

[6] M. Nocita, A. Stevens, B. van Wesemael, M. Aitkenhead, M. Bachmann, B. Barthès, E.B. Dor, D.J. Brown, M. Clairotte, A. Csorba, et al., Soil spectroscopy: an alternative to wet chemistry for soil monitoring, in: Advances in Agronomy, vol. 132, Elsevier, 2015, pp. 139–159.

[7] B. Ludwig, R. Murugan, V.R. Parama, M. Vohland, Use of different chemometric approaches for an estimation of soil properties at field scale with near infrared spectroscopy, J. Plant Nutr. Soil Sci. 181 (5) (2018) 704–713.

[8] R. Reda, T. Saffaj, B. Ilham, O. Saidi, K. Issam, L. Brahim, et al., A comparative study between a new method and other machine learning algorithms for soil organic carbon and total nitrogen prediction using near infrared spectroscopy, Chemometr. Intell. Lab. Syst. 195 (2019) 103873.

[9] A. Pudełko, M. Chodak, Estimation of total nitrogen and organic carbon contents in mine soils with NIR reflectance spectroscopy and various chemometric methods, Geoderma 368 (2020) 114306.

[10] M. Mancini, D.C. Weindorf, S. Chakraborty, S.H.G. Silva, A.F. dos Santos Teixeira, L.R.G. Guilherme, N. Curi, Tracing tropical soil parent material analysis via portable X-ray fluorescence (pXRF) spectrometry in Brazilian Cerrado, Geoderma 337 (2019) 718–728.

[11] S. Nawar, N. Delbecque, Y. Declercq, P. De Smedt, P. Finke, A. Verdoodt, M. Van Meirvenne, A.M. Mouazen, Can spectral analyses improve measurement of key soil fertility parameters with X-ray fluorescence spectrometry? Geoderma 350 (2019) 29–39.

[12] A. Rawal, S. Chakraborty, B. Li, K. Lewis, M. Godoy, L. Paulette, D.C. Weindorf, Determination of base saturation percentage in agricultural soils via portable X-ray fluorescence spectrometer, Geoderma 338 (2019) 375–382.

[13] A. Margenot, T. O'Neill, R. Sommer, V. Akella, Predicting soil permanganate oxidizable carbon (POXC) by coupling drift spectroscopy and artificial neural networks (ANN), Comput. Electron. Agric. 168 (2020) 105098.

[14] A. Sharma, D.C. Weindorf, D. Wang, S. Chakraborty, Characterizing soils via portable X-ray fluorescence spectrometer: 4. cation exchange capacity (CEC), Geoderma 239 (2015) 130–134.

[15] T.H. Dao, Instantaneous accounting for leaf water in X-ray fluorescence spectra of corn grown in manure-and fertilizer-amended soils, Comput. Electron. Agric. 129 (2016) 84–90.

[16] F. Morona, F.R. dos Santos, A.M. Brinatti, F.L. Melquiades, Quick analysis of organic matter in soil by energy-dispersive X-ray fluorescence and multivariate analysis, Appl. Radiat. Isot. 130 (2017) 13–20.

[17] Y. Declercq, N. Delbecque, J. De Grave, P. De Smedt, P. Finke, A.M. Mouazen, S. Nawar, D. Vandenberghe, M. Van Meirvenne, A. Verdoodt, A comprehensive study of three different portable XRF scanners to assess the soil geochemistry of an extensive sample dataset, Rem. Sens. 11 (21) (2019) 2490.

[18] A.F. dos Santos Teixeira, M.H.P. Pelegrino, W.M. Faria, S.H.G. Silva, M.G.M. Gonçalves, F.W.A. Júnior, L.R. Gomide, A.L.P. Júnior, I.A. de Souza, S. Chakraborty, et al., Tropical soil pH and sorption complex prediction via portable X-ray fluorescence spectrometry, Geoderma 361 (2020) 114132.

[19] D.C. Weindorf, N. Bakr, Y. Zhu, Advances in portable X-ray fluorescence (PXRF) for environmental, pedological, and agronomic applications, in: Advances in Agronomy, vol. 128, Elsevier, 2014, pp. 1–45.

[20] H. Borchani, G. Varando, C. Bielza, P. Larrañaga, A survey on multi-output regression, Wiley Interdiscipl. Rev.: Data Min. Knowl. Discov. 5 (5) (2015) 216–233.

[21] E. Spyromitros-Xioufis, G. Tsoumakas, W. Groves, I. Vlahavas, Multi-target regression via input space expansion: treating targets as inputs, Mach. Learn. 104 (1) (2016) 55–98.

[22] G. Melki, A. Cano, V. Kecman, S. Ventura, Multi-target support vector regression via correlation regressor chains, Inf. Sci. 415 (2017) 53–69.

[23] J.M. Moyano, E.L. Gibaja, S. Ventura, An evolutionary algorithm for optimizing the target ordering in ensemble of regressor chains, in: 2017 IEEE Congress on Evolutionary Computation (CEC), IEEE, 2017, pp. 2015–2021.

[24] S.M. Mastelini, E.J. Santana, V.G.T. da Costa, S. Barbon, Benchmarking multi-target regression methods, in: 2018 7th Brazilian Conference on Intelligent Systems (BRACIS), IEEE, 2018, pp. 396–401.

[25] D. Kocev, S. Džeroski, M.D. White, G.R. Newell, P. Griffioen, Using single- and multi-target regression trees and ensembles to model a compound index of vegetation condition, Ecol. Model. 220 (8) (2009) 1159–1168.

[26] S.B. Junior, S.M. Mastelini, A.P.A. Barbon, D.F. Barbin, R. Calvini, J.F. Lopes, A. Ulrici, Multi-target prediction of wheat flour quality parameters with near infrared spectroscopy, Inf. Process. Agric. 7 (2) (2020) 342–354.

[27] B. Liu, R. Wang, Z. Guan, J. Li, Z. Xu, X. Guo, Y. Wang, Improved support vector regression models for predicting rock mass parameters using tunnel boring machine driving data, Tunn. Undergr. Space Technol. 91 (2019) 102958.

[28] J. Padarian, B. Minasny, A. McBratney, Using deep learning to predict soil properties from regional spectral data, Geoderma Reg. 16 (2019), e00198.

[29] N.L. Tsakiridis, K.D. Keramaris, J.B. Theocharis, G.C. Zalidis, Simultaneous prediction of soil properties from VNIR-SWIR spectra using a localized multi-channel 1-D convolutional neural network, Geoderma 367 (2020) 114208.

[30] M.G. Tarnik, S. Ghafari, T. Bahraini, H.S. Yazdi, Minimum Variance Based-Bayes Combination for Prediction of Soil Properties on Vis-NIR Reflectance Spectroscopy, Chemometrics and Intelligent Laboratory Systems, 2020, p. 104194.

[31] L. Breiman, Stacked regressions, Mach. Learn. 24 (1) (1996) 49–64.

[32] S.B. Junior, E.J. Santana, A.T. Badaró, N.A. Borrás, D.F. Barbin, Advantages of multi-target modelling for spectral regression, in: Spectroscopic Techniques & Artificial Intelligence for Food and Beverage Analysis, Springer, 2020, pp. 95–121.

[33] E.J. Santana, S.M. Mastelini, S. Barbon Jr., Deep regressor stacking for air ticket prices prediction, in: XIII Brazilian Symposium on Information Systems: Information Systems for Participatory Digital Governance, Brazilian Computer Society (SBC), 2017, pp. 25–31.

[34] E.J. Santana, B.C. Geronimo, S.M. Mastelini, R.H. Carvalho, D.F. Barbin, E.I. Ida, S. Barbon, Predicting poultry meat characteristics using an enhanced multi-target regression method, Biosyst. Eng. 171 (2018) 193–204.

[35] J. Read, B. Pfahringer, G. Holmes, E. Frank, Classifier chains for multi-label classification, in: Joint European Conference on Machine Learning and Knowledge Discovery in Databases, Springer, 2009, pp. 254–269.
[36] S.M. Mastelini, V.G.T. da Costa, E.J. Santana, F.K. Nakano, R.C. Guido, R. Cerri, S. Barbon, Multi-output tree chaining: an interpretative modelling and lightweight multi-target approach, J. Signal Process. Syst. (2018) 1–25.
[37] G. Brown, J. Wyatt, R. Harris, X. Yao, Diversity creation methods: a survey and categorisation, Inf. Fusion 6 (1) (2005) 5–20.
[38] J. Mendes-Moreira, C. Soares, A.M. Jorge, J.F.d. Sousa, Ensemble approaches for regression: a survey, ACM Comput. Surv. 45 (1) (2012) 10.
[39] N.L. Tsakiridis, N.V. Tziolas, J.B. Theocharis, G.C. Zalidis, A genetic algorithm-based stacking algorithm for predicting soil organic matter from Vis-NIR spectral data, Eur. J. Soil Sci. 70 (3) (2019) 578–590.
[40] N. Rooney, D.W. Patterson, S.S. Anand, A. Tsymbal, Random subspacing for regression ensembles, in: FLAIRS Conference, vol. 2004, 2004.
[41] D.H. Wolpert, Stacked generalization, Neural Network. 5 (2) (1992) 241–259.
[42] H.L. Byers, L.J. McHenry, T.J. Grundl, XRF techniques to quantify heavy metals in vegetables at low detection limits, Food Chem. X 1 (2019) 100001.
[43] A. Khuder, M. Ahmad, R. Hasan, G. Saour, Improvement of X-ray fluorescence sensitivity by dry ashing method for elemental analysis of bee honey, Microchem. J. 95 (2) (2010) 152–157.
[44] M. Mantler, M. Schreiner, X-ray fluorescence spectrometry in art and archaeology, X-Ray Spectrometry, Int. J. 29 (1) (2000) 3–17.
[45] M.I.M.S. Bueno, M.T. Castro, A.M. de Souza, E.B.S. de Oliveira, A.P. Teixeira, X-ray scattering processes and chemometrics for differentiating complex samples using conventional EDXRF equipment, Chemometr. Intell. Lab. Syst. 78 (1–2) (2005) 96–102.
[46] D.C. Weindorf, Y. Zhu, S. Chakraborty, N. Bakr, B. Huang, Use of portable X-ray fluorescence spectrometry for environmental quality assessment of peri-urban agriculture, Environ. Monit. Assess. 184 (1) (2012) 217–227.
[47] C. Parsons, E.M. Grabulosa, E. Pili, G.H. Floor, G. Roman-Ross, L. Charlet, Quantification of trace arsenic in soils by field-portable X-ray fluorescence spectrometry: considerations for sample preparation and measurement conditions, J. Hazard Mater. 262 (2013) 1213–1222.
[48] F. Rodrigues dos Santos, E. de Almeida, P.D. da Cunha Kemerich, F.L. Melquiades, Evaluation of metal release from battery and electronic components in soil using SR-TXRF and EDXRF, X Ray Spectrom. 46 (6) (2017) 512–521.
[49] R. Van Grieken, A. Markowicz, Handbook of X-Ray Spectrometry, Marcel Dekker, New York, 2002.
[50] WRB, IUSS Working Group, World reference base for soil resources, update 2015, International Soil Classification System for Naming Soils and Creating Legends for Soil Maps, World Soil Resources Report, vol. 106, 2014.
[51] H.G.d. Santos, P.K.T. Jacomine, L.H. C.d. Anjos, V.A.d. Oliveira, J.B.d. Oliveira, M.R. Coelho, J.F. Lumbreras, T.J. F.d. Cunha, Sistema brasileiro de classificação de solos, Embrapa Solos, Rio de Janeiro, 2006.
[52] M.A. Pavan, M.d.F. Bloch, H.d.C. Zempulski, M. Miyazawa, D.C. Zocoler, Manual de análise química de solo e controle de qualidade, IAPAR Londrina, Londrina, 1992.
[53] M. Kaniu, K. Angeyo, A. Mwala, M. Mangala, Direct rapid analysis of trace bioavailable soil macronutrients by chemometrics-assisted energy dispersive X-ray fluorescence and scattering spectrometry, Anal. Chim. Acta 729 (2012) 21–25.
[54] B. Vandeginste, D. Massart, L. Buydens, S. De Jong, P. Lewi, J. Smeyers-Verbeke, Chapter 30 - cluster analysis, in: B. Vandeginste, D. Massart, L. Buydens, S. De Jong, P. Lewi, J. Smeyers-Verbeke (Eds.), Handbook of Chemometrics and Qualimetrics: Part B, Vol. 20 of Data Handling in Science and Technology, Elsevier, 1998, pp. 57–86.
[55] D. Elavarasan, D.R. Vincent, V. Sharma, A.Y. Zomaya, K. Srinivasan, Forecasting yield by integrating agrarian factors and machine learning models: a survey, Comput. Electron. Agric. 155 (2018) 257–282.
[56] R.V. Rossel, R. McGlynn, A. McBratney, Determining the composition of mineral-organic mixes using UV–vis–NIR diffuse reflectance spectroscopy, Geoderma 137 (1–2) (2006) 70–82.
[57] V. Bellon-Maurel, E. Fernandez-Ahumada, B. Palagos, J.-M. Roger, A. McBratney, Critical review of chemometric indicators commonly used for assessing the quality of the prediction of soil attributes by NIR spectroscopy, Trac. Trends Anal. Chem. 29 (9) (2010) 1073–1081.
[58] H. Zhou, Z. Deng, Y. Xia, M. Fu, A new sampling method in particle filter based on pearson correlation coefficient, Neurocomputing 216 (2016) 208–215.